CRISPR-Cas9 mediated *LAG*-3 disruption in CAR-T cells

Yongping Zhang[1], Xingying Zhang[2,3], Chen Cheng[2,4], Wei Mu[2,3], Xiaojuan Liu[2], Na Li[2], Xiaofei Wei[6], Xiang Liu[2], Changqing Xia (✉)[1,5,a], Haoyi Wang (✉)[2,3,b]

[1]*Department of Hematology, Xuanwu Hospital, Capital Medical University, Beijing 100053, China;* [2]*State Key Laboratory of Stem Cell and Reproductive Biology, Institute of Zoology, Chinese Academy of Sciences, Beijing100190, China;* [3]*University of Chinese Academy of Sciences, Beijing 100049, China;* [4]*Graduate School, University of Science and Technology of China, Hefei 230026, China;* [5]*Department of Pathology, Immunology and Laboratory Medicine, University of Florida, FL 32611, USA;* [6]*Beijing Cord Blood Bank, Beijing100176, China*

Abstract **T cells engineered with chimeric antigen receptor (CAR) have been successfully applied to treat advanced refractory B cell malignancy. However, many challenges remain in extending its application toward the treatment of solid tumors. The immunosuppressive nature of tumor microenvironment is considered one of the key factors limiting CAR-T efficacy. One negative regulator of T cell activity is lymphocyte activation gene-3 (*LAG-3*). We successfully generated *LAG-3* knockout T and CAR-T cells with high efficiency using CRISPR-Cas9 mediated gene editing and found that the viability and immune phenotype were not dramatically changed during *in vitro* culture. *LAG-3* knockout CAR-T cells displayed robust antigen-specific antitumor activity in cell culture and in murine xenograft model, which is comparable to standard CAR-T cells. Our study demonstrates an efficient approach to silence immune checkpoint in CAR-T cells via gene editing.**

Keywords CAR-T; CRISPR-Cas9; *LAG-3*

Introduction

Chimeric antigen receptor T (CAR-T) cell therapy has gained tremendous popularity as a promising treatment for cancer in recent years. As an artificial T cell receptor, CAR is composed of a single-chain variable fragment (scFv) derived from a monoclonal antibody recognizing an antigen, a transmembrane domain, and an intracellular domain derived from CD3Z and/or co-stimulatory molecules [1]. CAR-T cell therapy has been exceptionally successful in treating B cell acute lymphoblastic leukemia (B-ALL) in early phase clinical studies, with a complete response rate of 70%–90% [2–4]. However, the clinical response, when targeting other CD19-positive hematological malignancies such as chronic lymphoblastic leukemia (CLL), is less effective, with a response rate of approximately 50%. The reason for the low response rate was possibly because of the immune suppression through T cell checkpoint inhibitory receptors [5]. Similarly, the tumor immunosuppressive microenvironment (TME) poses serious challenge to CAR-T's efficacy when treating solid tumors.

The inhibitory pathways of the immune system that modulate immune responses are referred to as immune checkpoints, which are utilized by tumor to gain immune resistance, particularly by inhibiting tumor-specific T cells [6]. The cell surface protein LAG-3 is an important inhibitory receptor with structural homologies to CD4. The protein binds MHC class II molecules with a cell with higher affinity than CD4 [7,8]. LAG-3 also interacts with LSECT in a surface lectin of the DC-SIGN family, which is expressed on dendritic cells and also on tumor tissue [9]. *LAG-3* is expressed on activated CD4 and CD8 T cells, regulatory T cells (Tregs), natural killer (NK) cells, B cells, and plasmacytoid dendritic cells [9–15].

Accumulating evidence indicates that LAG-3 exhibits a negative impact on effector function of T cells *in vivo* and *in vitro* [9,16–18] and enhances the suppressive function of Treg cells [13,19]. As a T cell exhaustion marker, LAG-3 is upregulated in cancer and chronic infections [20,21]. LAG-3 blockade *in vitro* augments T cell proliferation and cytokine productions, leading to an increase in memory cells due to a delayed cell cycle arrest [22,23]. Dual blockade of PD-1 and LAG-3 reverses T cell exhaustion and improves therapeutic activity in preclinical models of chronic infection and cancers in a synergistic manner [20,21,24–28]. Clinical trials, which explore the use of

anti-LAG-3 antibodies either alone or in combination with anti-PD-1 in both solid and hematologic cancers, are in progress (ClinicalTrials.gov, numbers: NCT02061761, NCT01968109).

Permanently silencing immune checkpoint receptors, such as PD-1 and LAG-3 in CAR-T cells through gene editing *in vitro* before adoptive cell transfer, represents an exciting approach to improve the efficacy of CAR-T cells, while avoiding the potential toxicities associated with the long-term administration of anti-LAG-3 antibodies. While PD-1 has been eliminated from T cells using gene editing and showed elevated T cell function [29–32], human T and CAR-T cells with *LAG-3* knockout have not been described.

Clustered Regularly Interspaced Short Palindromic Repeats (CRISPR) and the CRISPR-associated protein (Cas) (CRISPR-Cas9) system is a powerful system for gene editing. We have established methods to disrupt single and multiple genes in CAR-T cells with high efficiency [30,31]. In this study, we eliminated *LAG-3* expression on human T and CAR-T cells using CRISPR-Cas9 and characterized the phenotype and functions of these modified cells.

Materials and methods

Primary human umbilical cord blood (UCB)-derived T cells

Fresh UCB units were obtained from the Beijing Cord Blood Bank (Beijing, China) with informed consent from healthy volunteer donors. After Histopaque-1077 (Sigma-Aldrich) gradient separation, mononuclear cells were collected, and T cells were isolated using the EasySep human T cell enrichment kit (Stemcell Technologies). T cells were stimulated with anti-CD3/CD28 Dynabeads (Thermo Fisher Scientific) at a bead to T cell ratio of 1:1 and cultured in X-vivo15 medium (Lonza) supplemented with 5% (v/v) heat-inactivated fetal bovine serum, 2 mmol/L L-glutamine, and 1 mmol/L sodium pyruvate in the presence of 300 IU/ml recombinant human IL-2 (all from Thermo Fisher Scientific).

Cell lines

K562 (erythroleukemia cell line) and Raji (Burkitt's lymphoma cell line) were purchased from American Type Culture Collection (ATCC). Raji-ffluc for biolumi-nescent imaging and K562-CD19 cells were generated as previously described [31]. All cell lines were grown under standard conditions in RPMI1640 medium (Thermo Fisher Scientific). Lentiviral producer cell lines 293T (ATCC-CRL3216) were maintained in DMEM (Thermo Fisher Scientific). All media were supplemented with 10% (v/v) fetal bovine serum, 100 U/ml penicillin and streptomycin, 2 mmol/L L-glutamine, and 1 mmol/L sodium pyruvate. All cell lines were grown at 37 °C in a 5% CO_2 atmosphere.

sgRNA design and *in vitro* T7 transcription of sgRNA

We obtained the first exon sequence of *LAG-3* from NCBI and used the CRISPR Design Tool (http://crispr.mit.edu) to design sgRNAs. Oligonucleotides containing T7 promoter and 20 bp targeting sequences were synthesized as forward primer (Supplementary Table S1). T7-sgRNA PCR product was amplified using pX330 plasmid (Addgene plasmid #4223) as template, column-purified, and used as the template for *in vitro* transcription using MEGAshort-script T7 kit (Thermo Fisher Scientific). RNAs were purified using MEGAclear columns (Thermo Fisher Scientific) and eluted in RNase-free water.

Generation of *LAG-3* knockout T cells

T cells were stimulated for 3 days, and then 1×10^6 cells were electroporated with 3 μg Cas9 protein (Thermo Fisher Scientific) and 3 μg sgRNAs targeting the *LAG-3* exon1 by 4D-Nucleofector System N (Lonza) using the P3 Primary Cell 4D-Nucleofector X Kit (V4XP-3024, Lonza) according to manufacturer instructions. Program EO-115 was used. After electroporation, cells were resuspended in 2 ml pre-warmed T cell medium and transferred into 12-well cell plate and incubated at 37 °C in 5% CO_2. The transfection efficiency was evaluated 3 days after electro-poration. Cell culture medium was half replaced by fresh complete medium every 2 days to 3 days. A similar procedure was used to generate *LAG-3* knockout CAR-T cells. Freshly purified primary T cells were activated for 1 day and then transduced with lentiviral vectors, harboring a second-generation CD19 CAR. The structure of the CAR was previously described [31]. Two days after transduction, CAR-T cells were electroporated with Cas9 protein and sgRNAs using the previously described procedure.

Flow cytometry

All samples were analyzed with CytoFLEX (Beckman Coulter Inc.) on the following days after transfection. The mouse anti-human antibodies to the following antigens were used: CD45RO-PE (UCHL1, Biolegend), CD45RA-PerCP/Cy5.5 (HI100, Biolegend), CD62L-Brilliant Vio-let421 (DREG-56, Biolegend), CD223 (LAG-3)-PE (11C3C65, Biolegend), CD8-APC (HIT8a, Biolegend), and CD4-PE (A161A1, Biolegend).

Sequencing of the mutations

Indels were quantified by TIDE (tracking of indels by decomposition) analysis and clonal sequence analysis. Cells were harvested, and the genomic DNA was extracted with 100 μg/ml proteinase K in lysis buffer (10 mmol/L Tris-HCl, 2 mmol/L EDTA, 2.5% Tween-20, and 2.5% Triton-X 100). The primers used for the amplification of target locus and sequencing are listed in Table S1. The PCR products were sequenced for TIDE analysis using web tool (available at http://tide.nki.nl). The purified PCR segments were cloned into pEASY vector using pEASY Blunt Cloning Kit (Transgen Biotech) to detect mutant alleles. A total of 40–70 colonies per sample of the transformed PCR ligation products are sequenced using universal primer M13F. All PCR sequencing methods used followed the instructions provided by the manufacturer or standard molecular cloning protocols.

Cytokine enzyme-linked immunosorbent assay (ELISA)

Cytokine release assays were performed by coculture of effector (CAR-T, LAG-3-KO-CAR-T, T) with target tumor cells (Raji, K19, K562) at a 1:1 ratio (10^4 cells each) per well, in duplicate in 96-well V-bottom plates, in a final volume of 200 μl complete RPMI1640 medium. After 24 h, supernatants were assayed to produce IL-2 and IFN-γ using ELISA kit (Biolegend).

Flow cytometry-based cytotoxicity assay

The cytotoxicity of the CAR-T cell was assessed by the flow cytometry-based cytotoxicity assay [31]. The lytic activities of effector cells were tested by Violet/Annexin V and 7-AAD labeling assay. Target tumor cells were labeled with 1 μmol/L Celltrace Violet and then incubated with effector cells by different effectors to target ratio for 4 h. FITC-Annexin V and 7-AAD (Biolegend) were added to determine the ratio of dead target cells. Samples were analyzed by flow cytometry. Target cells were selected by gating the Violet-positive cell population and further analyzed for different subpopulations. The percentages of cytotoxic activity were calculated using the following equation: % specific lysis = {[% ($Violet^+Annexin\ V^+$ + $Violet^+Annexin\ V^-7\text{-}AAD^+$) − % spontaneous ($Violet^+$ Annexin V^+ + $Violet^+Annexin\ V^-7\text{-}AAD^+$)]/[100% − % spontaneous ($Violet^+Annexin\ V^+$ + $Violet^+Annexin$ $V^-7\text{-}AAD^+$)]} × 100%.

Murine xenograft studies

To establish the Raji-ffluc tumor model, 6−12 weeks old NOD-Prkdcscid Il2rgnull (NPG) mice (VITALSTAR, Beijing, China) were injected with $2 × 10^5$ Raji-ffluc cells via intraperitoneal injection on day 0. Three days after injection, tumor engraftment was evaluated by serial biophotonic imaging using the NightOWL LB983 *in vivo* Imaging System (Berthold Technologies). Mice with comparable tumor loads were segregated into different treatment groups. T cells were administered at a dose of $1 × 10^7$ cells/mouse via intraperitoneal injection. The tumor loads were evaluated 7 days after treatment.

Results

Screening for the most efficient sgRNAs, targeting *LAG-3* in T cells

To achieve efficient gene disruption, we designed five sgRNAs, targeting the first exon of *LAG-3* (Table S1). The gene editing efficiency using each sgRNA was quantified by TIDE analysis [33], and the most efficient sgRNA (sgRNA5) was selected for further experiments (Fig. 1A and 1B). Gene editing using sgRNA5 in another donor-derived T cells achieved similar high *LAG-3* knockout efficiency (Fig. 1B). We amplified and sub-cloned the sgRNA5 target region and identified mutant alleles. A total of 30 out of 49 sequenced alleles are mutants, confirming the high gene disruption efficiency. As shown in Fig. 1C, all mutations recovered occurred precisely at the sgRNA targeting region. These results indicate that *LAG-3* can be efficiently eradicated in primary T cells.

Effect of electroporation and *LAG-3* knockout on T cell proliferation and phenotype

Next, the effect of *LAG-3* knockout on T cell proliferation and surface phenotype was determined. Upon anti-CD3 and anti-CD28 antibody stimulations, T cells with *LAG-3* knockout maintained normal proliferation (Fig. 2A). The immune phenotype of the gene-edited T cell was evaluated by the expression of CD4 and CD8, as well as the characteristics of naïve ($CD45RO^-$/$CD62L^+$, TN), central memory ($CD45RO^+$/$CD62L^+$, TCM), and effector memory ($CD45RO^+$/$CD62L^-$, TEM) T cell subsets. Compared with control T cells, a higher fraction of CD4 and TCM and a lower faction of CD8 cells were observed in *LAG-3* knockout T cells. However, this effect is probably caused by electroporation given that this feature was also observed in T cells receiving electroporation without Cas9 RNP (Fig. 2B). Overall, *LAG-3* knockout T cells displayed characteristics similar to non-edited T cells.

Off-target analysis

The potential off-target mutation is a major concern of CRISPR-Cas9 gene editing. The top five potential off-target sites for sgRNA5 were predicted using Benchling
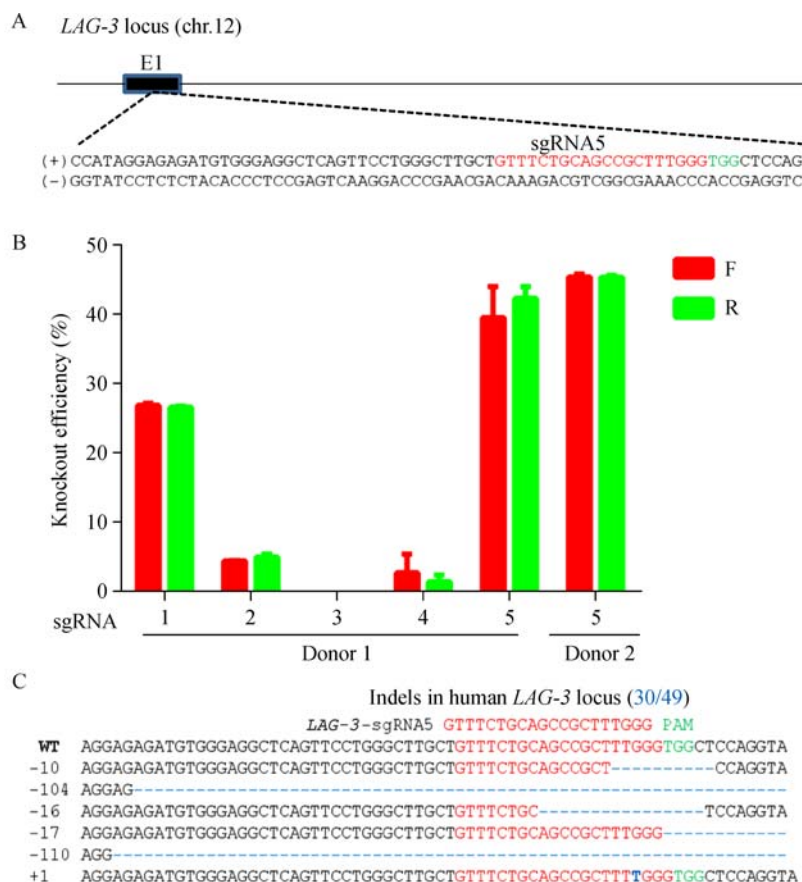
Fig. 1 Gene editing of *LAG-3* in human primary T cells using CRISPR-Cas9. (A) Schematic of sgRNA5 targeting site at *LAG-3* locus. The red color represents the sgRNA targeting sequence, and the green color represents the PAM sequence. (B) *LAG-3* knockout efficiency using different sgRNAs. Column plot shows the indel frequency (mean ± SEM, *n* = 2) of *LAG-3* analyzed by TIDE analysis using either forward (F) or reverse (R) sequencing primer. Experiments are performed in two biological replicates. (C) Representative mutant alleles in RNP-transfected cells compared with wild-type sequence (WT). sgRNA targeting sites are colored in red, PAM sequence in green, and mutations in blue; PCR products from each sample are sub-cloned, and each cloned allele was sequenced. 30/49 indicates the number of clones containing mutant alleles out of total clones sequenced.

software [34], and the five loci in the T cells with *LAG-3* knockout were genotyped (Table S1). We did not detect mutation at any of these loci using TIDE analysis (Table S2).

Preparation and characterization of *LAG-3* knockout CD19 CAR-T cells

CD19 is presented in most B cell malignancies, and anti-CD19 CAR-T cells were best characterized and successfully applied to treating CD19⁺ B cell leukemia and lymphomas [2–4]. We successfully generated *LAG-3* knockout anti-CD19 CAR-T cells, and *LAG-3* knockout efficiency is approximately 45%–70% in CAR-T cells produced from three different donors (Fig. 3A and 3B). Loss of LAG-3 function was confirmed by detecting LAG-3 protein expression using flow cytometry (Fig. 3C). The

CAR-T cells electroporated with Cas9 RNP effectively proliferated. However, we did not observe much robust cell proliferation in *LAG-3* knockout CAR-T cells compared to control cells (Fig. 3D).

The surface expression of *LAG-3* is low after expansion; thus, performing enrichment for *LAG-3* knockout CAR-T cells is difficult. Therefore, the prepared *LAG-3* knockout CAR-T cells are a mixture of cells with and without *LAG-3* mutations. Samples from donors 2 and 3 with *LAG-3* knockout efficiency of more than 70% were used for the following functional analysis (Fig. 3A).

***In vitro* characterization of *LAG-3* knockout CD19 CAR-T cells**

To characterize CAR-T cells with *LAG-3* disruption phenotypically, we harvested CAR-T cells on day 14
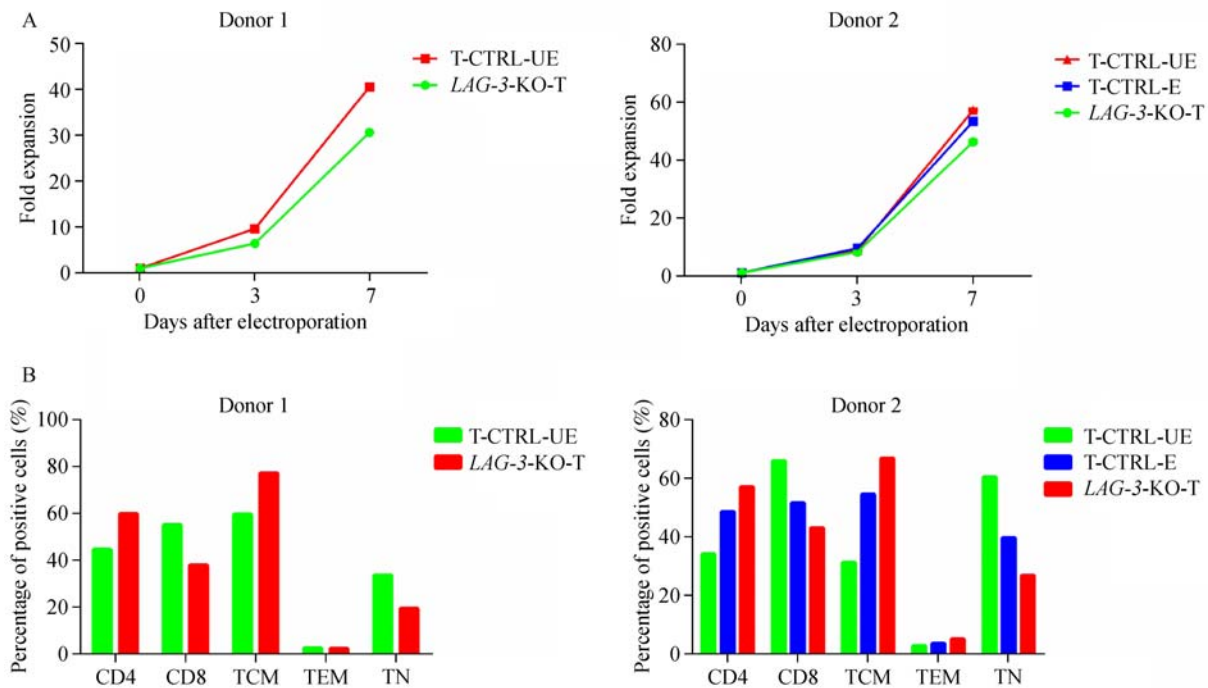
Fig. 2 Analysis of proliferation and phenotype of *LAG-3* knockout T cells. (A) Fold expansion of control and *LAG-3* knockout T cells. Total cell numbers were counted on days 3 and 7. (B) Immunophenotype of the gene-edited T cell was assessed 10 days after electroporation by the expression of CD4 and CD8, as well as the characteristics of naïve (CD45RO$^-$/CD62L$^+$, TN), central memory (CD45RO$^+$/CD62L$^+$, TCM), and effector memory (CD45RO$^+$ /CD62L$^-$, TEM) T cell subsets. Data shown are mean $\pm$ SEM of two independent experiments. T-CTRL-UE and T-CTRL-E indicate T cells with or without mock electroporation, and *LAG-3*-KO-T indicates RNP-treated T cells.

post transfection. Similar to the primary T cells, the *LAG-3* knockout CAR-T cells did not show major change in the expression of CD4 and CD8 as well as the memory T cell phenotypic features compared with control CAR-T cells electroporated without Cas9 RNP (Fig. 4A). Consistent with the results in T cells, these data suggest that although electroporation has some effect, CRISPR-Cas9-mediated *LGA-3* disruption does not interfere with the immunophenotype of CAR-T cells.

The cytotoxic function of *LAG-3* knockout CAR-T cells was first evaluated using *in vitro* culture. Similar to standard CAR-T cells, *LAG-3* knockout CAR-T cells released IL-2 and IFN-γ only when they were cocultured with CD19-expressing Raji or K562-CD19 cells (Fig. 4B). This cytokine release was dependent on CAR given that non-transduced T cells failed to release cytokines in the presence of CD19 positive cells. Furthermore, the amount of cytokines released by *LAG-3* knockout CAR-T cells is similar to standard CAR-T cells (Fig. 4B). In cytotoxicity assay, *LAG-3* knockout CAR-T cells showed CAR-dependent lysis of CD19 tumor targets (Fig. 4C). These results indicate that CAR-T cells with *LAG-3* disruption maintain antitumor activity equivalent to standard CAR-T cells.

LAG-3 knockout CD19 CAR-T cells eradicate tumor in murine xenograft model

To further evaluate the antitumor function of the *LAG-3* knockout CAR-T cells, we employed Raji-ffluc lymphoma xenograft models. Except for one mouse (likely due to technical error) in CAR-T treated group, tumor size was substantially smaller in all mice treated with standard CAR-T cells and *LAG-3* knockout CAR-T cells, whereas progressive tumor growth was observed in the control group of mice treated with un-modified T cells or PBS (Fig. 5A and 5B). The survival of mice that received *LAG-3* knockout and standard CAR-T cells is also longer (Fig. 5C). The tumor burden of mice treated with standard CAR-T and *LAG-3* knockout CAR-T was similar, indicating that CAR-T cells with and without *LAG-3* disruption have similar antitumor efficacy in this Raji-ffluc lymphoma murine xenograft model.

To evaluate the engraftment of CAR-T cells *in vivo*, we sacrificed one of the *LAG-3* knockout CAR-T cells treated mice 71 days after treatment, and no tumor was detectable. The peripheral blood, peritoneal wash fluid, and spleen cells were collected, and human T cells and CAR-T cells were detected using flow cytometry. As shown in Fig. S1,
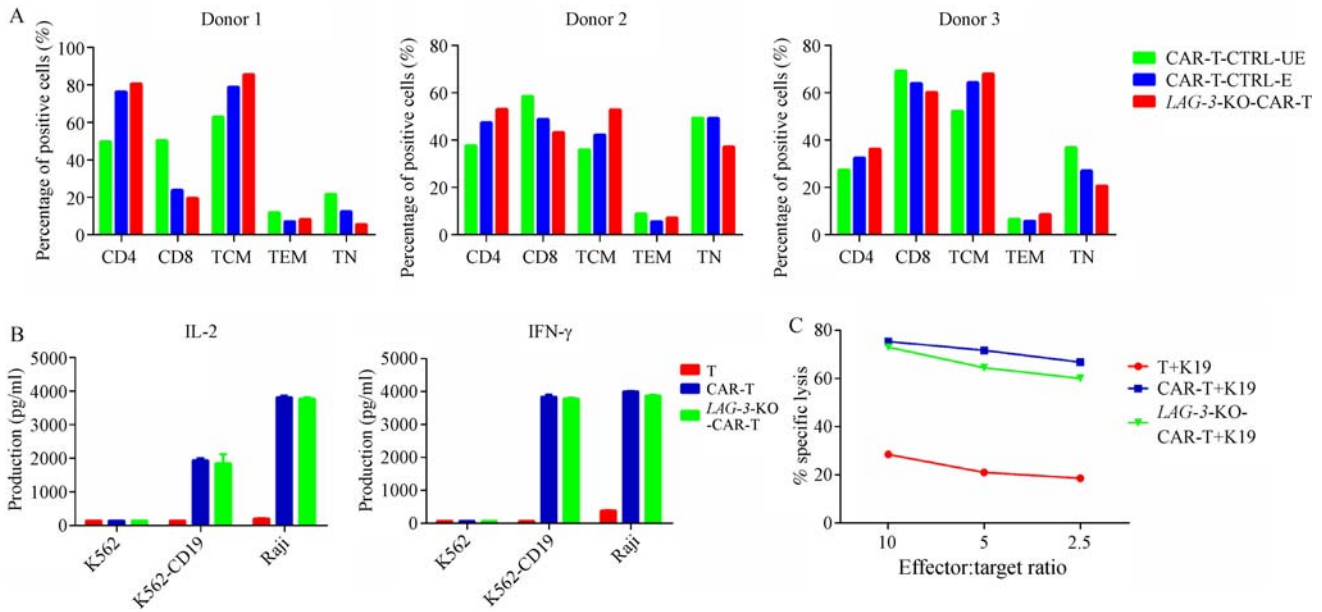
Fig. 3 Generation of *LAG-3* knockout CAR-T cells. (A) *LAG-3* knockout efficiency in CAR-T cells from three donors. (B) Representative sequences of mutated alleles in RNP-transfected CAR-T cells compared with wild-type CAR-T sequence (WT). sgRNA targeting sites are colored in red, PAM sequence in green, and mutations in blue; 60/71 indicates the number of clones containing mutant alleles out of total clones sequenced. (C) Flow cytometric analysis (mean ± SEM, $n = 2$) of *LAG-3* surface expression of control and *LAG-3*-KO-CAR-T cells from two donors, at day 3 post-electroporation. (D) Fold expansion (mean ± SEM, $n = 2$) of RNP-treated CAR-T cells and control CAR-T cells from three donors. Data shown are mean ± SEM of two independent experiments. CAR-T-CTRL-UE and CAR-T-CTRL-E indicate T cells with or without mock electroporation, and *LAG-3*-KO-CAR-T indicates RNP-treated cells.

extremely limited human T and CAR-T cells were found in mouse peripheral blood, whereas some human T and CAR-T cells exist in the peritoneal cavity and spleen, indicating that these cells can achieve long-term engraftment *in vivo*.

Discussion

With a complete response rate of 70%–90% [2–4], CAR-T therapy offers an effective treatment for B cell acute lymphoblastic leukemia. Building on this success, efforts are ongoing to extend it toward the treatment of solid tumors; however, the clinical response is extremely limited [1]. Recent studies suggest that CAR-T cells and endogenous T cells are likely to suffer the loss of cytotoxic functionality in immunosuppressive tumor microenvironment [6]. Strategies that improve the efficacy of CAR-T cells, by preventing the negative regulation of effector functions mediated by the immunosuppressive tumor

microenvironment, are critical for solid tumor immunotherapy. The well-known features and functions of *LAG-3* allow it to be an attractive target for immune modulation.

To this end, we described, for the first time, the disrupting *LAG-3* expression in human primary T cells and CAR-T cells using CRISPR-Cas9 system. We demonstrate that the delivery of CRISPR-Cas9 system via electroporation provides an efficient platform to knockout *LAG-3* in T and CAR-T cells. Different from *in vivo* study using mouse model [22], we did not find any significant difference in the cell expansion rate between *LAG-3* knockout cells and control cells. In addition, the *LAG-3* knockout CAR-T cells were not adversely affected by the electroporation process and were rich in central memory subtype. *LAG-3* knockout CAR-T cells maintained their antigen-specific cytokine release and antitumor potency *in vitro* and *in vivo*.

Previous studies demonstrated that the blockade of *LAG-3* by monoclonal antibody enhanced cytokine release

Fig. 4 *In vitro* characterization of *LAG-3* knockout CD19 CAR-T cells. (A) Immunophenotype of the gene-edited CAR-T cell was assessed 10 days after electroporation by the expression of CD4 and CD8 as well as the characteristics of naïve, central memory, and effector memory T cell subsets. Data shown are mean ± SEM of three independent experiments. (B) IL-2 and IFN-γ production (mean ± SEM, $n = 2$). (C) Cytotoxicity assay evaluating the cell lytic activity of T, CAR-T, and *LAG-3*-KO-CAR-T cells against K19 cells.
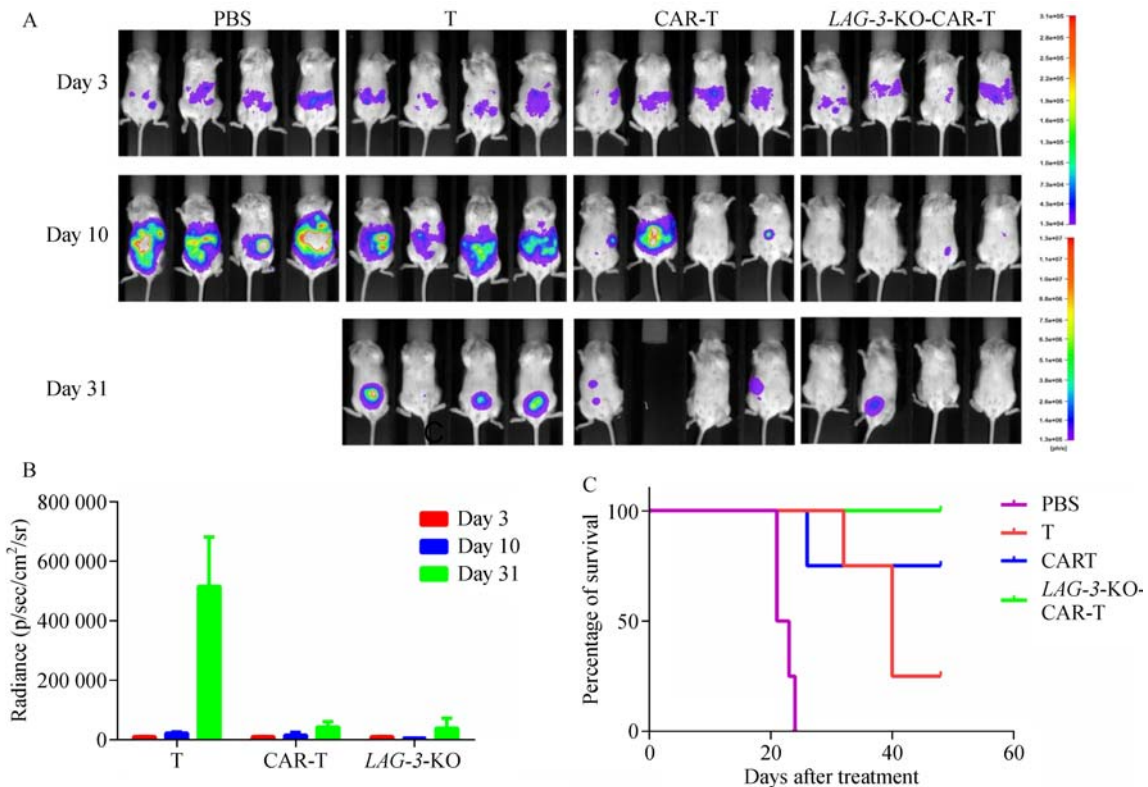
Fig. 5 Evaluation of the antitumor activity of *LAG-3* knockout CAR-T cells *in vivo*. On day 0, NPG mice were injected intraperitoneally with 2×10^5 Raji-luciferase cells. On day 3, mice received 1×10^7 CAR-T cells, *LAG-3*-KO-CAR-T cells, T cells, or PBS intraperitoneally. (A) Bioluminescent imaging result of NPG mice treated with CAR-T and *LAG-3*-KO-CAR-T cells on days 3, 10, and 31 ($n = 4$). (B) Bioluminescent signal (mean ± SEM, $n = 4$) of NPG mice treated with CAR-T cells, *LAG-3*-KO-CAR-T cells, and T cells. (C) Survival curve of 50-day post treatment.

and cytoxicity *in vivo* and *in vitro* [9,16–18]. The present study did not find a positive effect on CAR-T effector function following *LAG-3* disruption. One possibility is that our murine tumor model does not recapitulate primary tumor immunosuppressive environment. Therefore, *LAG-3*-disrupted CAR-T cells do not show advantage of resisting T cell exhaustion. In addition, LAG-3 and PD-1 work in a synergetic manner; thus, only blocking *LAG-3* function might not be sufficient to show superior efficacy [25]. Therefore, future efforts are required to explore *PD-1* and *LAG-3* double knockout CAR-T cells, which are evaluated in a murine model with better TME setup, such as PDX model. We only achieved ~70% *LAG-3* knockout efficiency; thus, the remaining 30% WT cells might also affect the functional evaluations.

In conclusion, we established a CRISPR-Cas9-based method for highly efficient disruption of *LAG-3* in human primary T cells and CAR-T cells. While the potential advantages of *LAG-3* knockout CAR-T cells require further study, using gene editing to silence immune check points promises to improve the efficacy of CAR-T cells treating solid tumors.

Acknowledgements

Compliance with ethics guidelines

Yongping Zhang, Xingying Zhang, Chen Cheng, Wei Mu, Xiaojuan Liu, Na Li, Xiaofei Wei, Xiang Liu, Changqing Xia, and Haoyi Wang declare that they have no conflict of interest. All procedures followed were in accordance with the ethical standards of the responsible committee on human experimentation (institutional and national) and with the *Helsinki Declaration* of 1975, as revised in 2000. Informed consent was obtained from all healthy donors for being included in the study. All institutional and national guidelines for the care and use of laboratory animals were followed.

Electronic Supplementary Material Supplementary material is available in the online version of this article at http://dx.doi.org/10.1007/s11684-017-0543-6 and is accessible for authorized users.

References

1. Kakarla S, Gottschalk S. CAR T cells for solid tumors: armed and ready to go? Cancer J 2014; 20(2): 151–155

2. Davila ML, Riviere I, Wang X, Bartido S, Park J, Curran K, Chung SS, Stefanski J, Borquez-Ojeda O, Olszewska M, Qu J, Wasielewska T, He Q, Fink M, Shinglot H, Youssif M, Satter M, Wang Y, Hosey J, Quintanilla H, Halton E, Bernal Y, Bouhassira DC, Arcila ME, Gonen M, Roboz GJ, Maslak P, Douer D, Frattini MG, Giralt S, Sadelain M, Brentjens R. Efficacy and toxicity management of 19-28z CAR T cell therapy in B cell acute lymphoblastic leukemia. Sci Transl Med 2014; 6(224): 224ra25

3. Maude SL, Frey N, Shaw PA, Aplenc R, Barrett DM, Bunin NJ, Chew A, Gonzalez VE, Zheng Z, Lacey SF, Mahnke YD, Melenhorst JJ, Rheingold SR, Shen A, Teachey DT, Levine BL, June CH, Porter DL, Grupp SA. Chimeric antigen receptor T cells for sustained remissions in leukemia. N Engl J Med 2014; 371(16): 1507–1517

4. Lee DW, Kochenderfer JN, Stetler-Stevenson M, Cui YK, Delbrook C, Feldman SA, Fry TJ, Orentas R, Sabatino M, Shah NN, Steinberg SM, Stroncek D, Tschernia N, Yuan C, Zhang H, Zhang L, Rosenberg SA, Wayne AS, Mackall CL. T cells expressing CD19 chimeric antigen receptors for acute lymphoblastic leukaemia in children and young adults: a phase 1 dose-escalation trial. Lancet 2015; 385(9967): 517–528

5. McClanahan F, Riches JC, Miller S, Day WP, Kotsiou E, Neuberg D, Croce CM, Capasso M, Gribben JG. Mechanisms of PD-L1/PD-1-mediated CD8 T-cell dysfunction in the context of aging-related immune defects in the Eμ-TCL1 CLL mouse model. Blood 2015; 126(2): 212–221

6. Khalil DN, Smith EL, Brentjens RJ, Wolchok JD. The future of cancer treatment: immunomodulation, CARs and combination immunotherapy. Nat Rev Clin Oncol 2016; 13(5): 273–290

7. Triebel F, Jitsukawa S, Baixeras E, Roman-Roman S, Genevee C, Viegas-Pequignot E, Hercend T. LAG-3, a novel lymphocyte activation gene closely related to CD4. J Exp Med 1990; 171(5): 1393–1405

8. Huard B, Prigent P, Tournier M, Bruniquel D, Triebel F. CD4/major histocompatibility complex class II interaction analyzed with CD4- and lymphocyte activation gene-3 (LAG-3)-Ig fusion proteins. Eur J Immunol 1995; 25(9): 2718–2721

9. Xu F, Liu J, Liu D, Liu B, Wang M, Hu Z, Du X, Tang L, He F. LSECtin expressed on melanoma cells promotes tumor progression by inhibiting antitumor T-cell responses. Cancer Res 2014; 74(13): 3418–3428

10. Baixeras E, Huard B, Miossec C, Jitsukawa S, Martin M, Hercend T, Auffray C, Triebel F, Piatier-Tonneau D. Characterization of the lymphocyte activation gene 3-encoded protein. A new ligand for human leukocyte antigen class II antigens. J Exp Med 1992; 176(2): 327–337

11. Huard B, Gaulard P, Faure F, Hercend T, Triebel F. Cellular expression and tissue distribution of the human LAG-3-encoded protein, an MHC class II ligand. Immunogenetics 1994; 39(3): 213–217

12. Workman CJ, Rice DS, Dugger KJ, Kurschner C, Vignali DA. Phenotypic analysis of the murine CD4-related glycoprotein, CD223 (LAG-3). Eur J Immunol 2002; 32(8): 2255–2263

13. Huang CT, Workman CJ, Flies D, Pan X, Marson AL, Zhou G, Hipkiss EL, Ravi S, Kowalski J, Levitsky HI, Powell JD, Pardoll DM, Drake CG, Vignali DA. Role of LAG-3 in regulatory T cells. Immunity 2004; 21(4): 503–513

14. Kisielow M, Kisielow J, Capoferri-Sollami G, Karjalainen K. Expression of lymphocyte activation gene 3 (LAG-3) on B cells is induced by T cells. Eur J Immunol 2005; 35(7): 2081–2088

15. Workman CJ, Wang Y, El Kasmi KC, Pardoll DM, Murray PJ, Drake CG, Vignali DA. LAG-3 regulates plasmacytoid dendritic cell homeostasis. J Immunol 2009; 182(4): 1885–1891

16. Hannier S, Triebel F. The MHC class II ligand lymphocyte activation gene-3 is co-distributed with CD8 and CD3-TCR molecules after their engagement by mAb or peptide-MHC class I complexes. Int Immunol 1999; 11(11): 1745–1752

17. Workman CJ, Dugger KJ, Vignali DA. Cutting edge: molecular analysis of the negative regulatory function of lymphocyte activation gene-3. J Immunol 2002; 169(10): 5392–5395

18. Sierro S, Romero P, Speiser DE. The CD4-like molecule LAG-3, biology and therapeutic applications. Expert Opin Ther Targets 2011; 15(1): 91–101

19. Okamura T, Fujio K, Shibuya M, Sumitomo S, Shoda H, Sakaguchi S, Yamamoto K. $CD4^+CD25^-LAG3^+$ regulatory T cells controlled by the transcription factor Egr-2. Proc Natl Acad Sci USA 2009; 106 (33): 13974–13979

20. Wherry EJ, Ha SJ, Kaech SM, Haining WN, Sarkar S, Kalia V, Subramaniam S, Blattman JN, Barber DL, Ahmed R. Molecular signature of $CD8^+$ T cell exhaustion during chronic viral infection. Immunity 2007; 27(4): 670–684

21. Matsuzaki J, Gnjatic S, Mhawech-Fauceglia P, Beck A, Miller A, Tsuji T, Eppolito C, Qian F, Lele S, Shrikant P, Old LJ, Odunsi K. Tumor-infiltrating NY-ESO-1-specific $CD8^+$ T cells are negatively regulated by LAG-3 and PD-1 in human ovarian cancer. Proc Natl Acad Sci USA 2010; 107(17): 7875–7880

22. Workman CJ, Cauley LS, Kim IJ, Blackman MA, Woodland DL, Vignali DA. Lymphocyte activation gene-3 (CD223) regulates the size of the expanding T cell population following antigen activation *in vivo*. J Immunol 2004; 172(9): 5450–5455

23. Maçon-Lemaître L, Triebel F. The negative regulatory function of the lymphocyte-activation gene-3 co-receptor (CD223) on human T cells. Immunology 2005; 115(2): 170–178

24. Blackburn SD, Shin H, Haining WN, Zou T, Workman CJ, Polley A, Betts MR, Freeman GJ, Vignali DA, Wherry EJ. Coregulation of $CD8^+$ T cell exhaustion by multiple inhibitory receptors during chronic viral infection. Nat Immunol 2009; 10(1): 29–37

25. Richter K, Agnellini P, Oxenius A. On the role of the inhibitory receptor LAG-3 in acute and chronic LCMV infection. Int Immunol 2010; 22(1): 13–23

26. Butler NS, Moebius J, Pewe LL, Traore B, Doumbo OK, Tygrett LT, Waldschmidt TJ, Crompton PD, Harty JT. Therapeutic blockade of PD-L1 and LAG-3 rapidly clears established blood-stage Plasmodium infection. Nat Immunol 2011; 13(2): 188–195

27. Woo SR, Turnis ME, Goldberg MV, Bankoti J, Selby M, Nirschl CJ, Bettini ML, Gravano DM, Vogel P, Liu CL, Tangsombatvisit S, Grosso JF, Netto G, Smeltzer MP, Chaux A, Utz PJ, Workman CJ, Pardoll DM, Korman AJ, Drake CG, Vignali DA. Immune inhibitory molecules LAG-3 and PD-1 synergistically regulate T-cell function to promote tumoral immune escape. Cancer Res 2012; 72(4): 917–927

28. Goding SR, Wilson KA, Xie Y, Harris KM, Baxi A, Akpinarli A, Fulton A, Tamada K, Strome SE, Antony PA. Restoring immune function of tumor-specific $CD4^+$ T cells during recurrence of melanoma. J Immunol 2013; 190(9): 4899–4909

29. Menger L, Sledzinska A, Bergerhoff K, Vargas FA, Smith J, Poirot L, Pule M, Hererro J, Peggs KS, Quezada SA. TALEN-mediated inactivation of PD-1 in tumor-reactive lymphocytes promotes intratumoral T-cell persistence and rejection of established tumors. Cancer Res 2016; 76(8): 2087–2093

30. Ren J, Liu X, Fang C, Jiang S, June CH, Zhao Y. Multiplex genome editing to generate universal CAR T cells resistant to PD1 inhibition. Clin Cancer Res 2017 ; 23(9): 2255–2266

31. Liu X, Zhang Y, Cheng C, Cheng AW, Zhang X, Li N, Xia C, Wei X, Liu X, Wang H. CRISPR-Cas9-mediated multiplex gene editing in CAR-T cells. Cell Res 2017; 27(1): 154–157

32. Su S, Hu B, Shao J, Shen B, Du J, Du Y, Zhou J, Yu L, Zhang L, Chen F, Sha H, Cheng L, Meng F, Zou Z, Huang X, Liu B. Corrigendum: CRISPR-Cas9 mediated efficient PD-1 disruption on human primary T cells from cancer patients. Sci Rep 2017; 7: 40272

33. Brinkman EK, Chen T, Amendola M, van Steensel B. Easy quantitative assessment of genome editing by sequence trace decomposition. Nucleic Acids Res 2014; 42(22): e168

34. Hsu PD, Scott DA, Weinstein JA, Ran FA, Konermann S, Agarwala V, Li Y, Fine EJ, Wu X, Shalem O, Cradick TJ, Marraffini LA, Bao G, Zhang F. DNA targeting specificity of RNA-guided Cas9 nucleases. Nat Biotechnol 2013; 31(9): 827–832